Cluster-cluster aggregation in binary mixtures

A. AlSunaidi,[1,2] M. Lach-hab,[1] Agustín E. González,[3,*] and Estela Blaisten-Barojas[1,†]
[1]*Institute for Computational Sciences and Informatics, George Mason University, Fairfax, Virginia 22030*
[2]*Institue for Physical Science and Technology, University of Maryland, College Park, Maryland 20742*
[3]*Centro de Ciencias Físicas, Universidad Nacional Autónoma de México, Apartado Postal 48-3, Cuernavaca, Morelos 62251, Mexico*
(Received 17 June 1999)

The structure and aggregation kinetics of three-dimensional clusters composed of two different monomeric species at three concentrations are thoroughly investigated by means of extensive, large-scale computer simulations. The aggregating monomers have all the same size and occupy the cells of a cubic lattice. Two bonding schemes are considered: (a) the binary diffusion-limited cluster-cluster aggregation (BDLCA) in which only the monomers of different species stick together, and (b) the invading binary diffusion-limited cluster-cluster aggregation (IBDLCA) in which additionally monomers of one of the two species are allowed to bond. In the two schemes, the mixed aggregates display self-similarity with a fractal dimension d_f that depends on the relative molar fraction of the two species and on concentration. At a given concentration, when this molar fraction is small, d_f approaches a value close to the reaction-limited cluster-cluster aggregation of one-component systems, and when the molar fraction is 0.5, d_f becomes close to the value of the diffusion-limited cluster-cluster aggregation model. The crossover between these two regimes is due to a time-decreasing reaction probability between colliding particles, particularly at small molar fractions. Several dynamical quantities are studied as a function of time. The number of clusters and the weight-average cluster size display a power-law behavior only at small concentrations. The dynamical exponents are obtained for molar fractions above 0.3 but not at or below 0.2, indicating the presence of a critical transition between a gelling to a nongelling system. The cluster-size distribution function presents scaling for molar fractions larger than 0.2.

PACS number(s): 61.43.Hv, 82.70.Dd, 82.70.Gg, 05.10.Ln

I. INTRODUCTION

The structure and kinetics of aggregating colloids have been extensively studied, particularly in the past two decades [1–3]. Surprisingly, the theoretical study of irreversible aggregation between polydisperse particles and, more importantly, between colloids of two or more different species is scarce [4–7]. Compared to the aggregation of one-component systems, the coagulation of particles belonging to two or more species is a more common process in nature. For example, in geophysical systems there are minerals in which one of the constituents undergoes aggregation while the others remain stable. In the biological realm there are many examples, such as the antibody-antigen reaction [8], in which we have the existence of different aggregating species. The kinetics of the growth processes with different chemical compounds by itself is also of interest in aerosol science [9], where composite aerogels are investigated as novel nanoscale materials for chemical, electronic, and optical applications [10]. In other systems such as mixtures of stable and unstable colloids, the aggregation of the unstable component is strongly hindered by the presence of the stable particles. It would be of interest to study the dynamics of the aggregation of the unstable component [11].

The present study investigates the three-dimensional aggregation behavior of a system constituted of two types of colloidal monomers A and B of identical size. Two models are introduced. The first model is the binary diffusion-limited cluster-cluster aggregation (BDLCA), in which a molar fraction x of species A interacts with the molar fraction $(1-x)$ of species B with a sticking probability $p_{AB}=1$, whereas the particles A or B do not stick to other particles of the same species. The probabilities are $p_{AA}=0$ and $p_{BB}=0$. In the second model, the invading binary diffusion-limited cluster-cluster aggregation (IBDLCA), a molar fraction $1-x$ of invading impurities B that do not stick between themselves ($p_{BB}=0$) but stick to the A monomers, alters the aggregation of the A monomers. In this case $p_{AA}=1$ and $p_{AB}=1$. The work of Meakin and Djordjević [4] addresses aggregation in two-monomer systems containing particles and clusters of size s with size-independent mobility at one fixed volume fraction [the diffusion coefficient was taken as $D(s)\sim s^{\delta}$ with $\delta=0$]. In their work, several functionalities are associated to the two monomers, and the case A_6+B_6 is similar to BDLCA. These were pioneer simulations using 10 000 monomers at a volume fraction of 0.0048. The work of Stoll and Pefferkorn [6] referred to heterocoagulation of two types of colloids with different aggregation abilities. Kinetic results from these authors pertain to very small systems of only 1000 monomers at a volume fraction 0.0034. Because of the small system size, the aggregation times studied were too short to extract reasonable conclusions concerning the dynamical quantities. One of their cases corresponding to equal reactivity for all cluster sizes is equivalent to the A_6+B_6 case of Meakin and Djordjević [4]. The difference between these two works resides in the criterion to account for the time associated to sequential selection of monomers or clusters that are moved during the simulation. In our work we have generalized the dynamical approach by allowing size-dependent mobilities, we have scaled up the system to about half a million initial monomers, and we have considered three different volume fractions (0.01,0.03,0.05). By allowing size-dependent mobilities to the various clusters

*Electronic address: agustin@fenix.ifisicacu.unam.mx
†Electronic address: eblaiste@gmu.edu

$[D(R_g) \sim 1/R_g$, where R_g is the radius of gyration of the cluster], the kinetic and time-dependent behavior of the binary mixture quantities is more realistic [12] and prone to provide a better theoretical framework for comparison with quantities measured by experimentalists. By scaling up the simulations to contain two orders of magnitude more particles, we are ensuring that the aggregates are fractals described with one dimensionality as well as increasing the aggregation time to reach a regime where dynamical exponents and scaling are clearly detected. Finally, by considering several volume fractions we are able to predict the dependence of structural and dynamical quantities of our BDLCA and IBDLCA models on volume fraction, which is another important experimental variable [13,14].

This paper is organized as follows. Section II describes the algorithm used to perform the simulations of the BDLCA and IBDLCA models and includes the expressions used to compute the particle-particle reaction probabilities. In Sec. III we demonstrate that the clusters generated in the simulations at the various concentrations used are fractal, using a recently developed criterion [15–18]. This section contains our results for the d_f as a function of molar fraction of species A and as a function of volume fraction. In Sec. IV, we report our results for the kinetic and dynamical quantities, including the time dependence of the different moments of the cluster-size distribution, the associated exponents, and the scaling of the function describing the temporal change of the number of clusters of a given size. Finally, Sec. V concludes this work with a discussion and several concluding remarks.

II. MODEL AND METHODS

A system composed of a mixture of N_A and N_B different colloidal monomers of equal size is distributed at random on the cells of a simple-cubic lattice. Three concentrations ϕ of the N_A+N_B monodisperse unaggregated particles are considered: 0.01, 0.03, and 0.05, corresponding to cubic box sizes of 360, 250, and 210, respectively. Therefore, at each concentration the system contained about 470 000 monomers. The molar fraction of the A monomers, $x=N_A/(N_A+N_B)$, is a variable in our simulations. For each of the concentrations and each molar fraction x, 50 simulations were performed.

The aggregation process starts by selecting at random a monomer of species A or B. This monomer is then moved one lattice spacing on a random direction in the cubic lattice. A diffusion coefficient $D_{\max}$ is characteristic of the motion of either monomers A or B. When monomers A and B become nearest neighbors on the lattice, they stick with probability $p_{AB}=1$. On the other hand, monomers B do not stick among themselves even if they are nearest neighbors on the lattice ($p_{BB}=0$). Two different situations may arise when two A monomers are nearest neighbors: (i) The A monomers do not stick, $p_{AA}=0$, in which case the aggregation is called *binary diffusion limited cluster-cluster aggregation* (BDLCA); (ii) the A monomers stick between themselves, $p_{AA}=1$, and the model is called *invading binary diffusion-limited cluster-cluster aggregation* (IBDLCA).

The aggregation proceeds when two monomers encounter and stick forming a mixed cluster AB of size $s=2$ in BDLCA and IBDLCA, or a dimer AA in IBDLCA. The system is not monodisperse any longer. Clusters of size two move slower than the monomers. To take into account this effect, a cluster selected at random will move only if a random number X, uniformly distributed between $0<X<1$, satisfies $X<D(R_g)/D_{\max}$, where $D(R_g)\equiv 1/R_g$ is the diffusion coefficient for the selected cluster. Every time a cluster is selected, the Monte Carlo time is incremented by $1/N_C$, where N_C is the number of clusters at that time, regardless of whether the cluster would have been moved or not. As the aggregation proceeds and when two clusters encounter each other, they stick (forming a larger cluster) or not depending upon the type of monomers touched in the encounter. This process is continued until the clusters in the aggregation bath organize themselves into a floc, a short time before gelation.

III. STRUCTURAL PROPERTIES OF BDLCA AND IBDLCA AGGREGATES

The structure of a diffusion-grown aggregate is usually characterized by one unique fractal dimension, d_f. However, this might not be the case, and multifractality might be at issue [15]. An aggregate is statistically self-similar if its structural characteristics are the same at all length scales of observation, sufficiently larger than the size of the individual components. If this is the case, then only one fractal dimension is enough to describe the fractal characteristics of the aggregates in the final floc. Because of the complex nature of the reaction between monomers in our binary mixed aggregates, it is instructive to show that the clusters generated in BDLCA and IBDLCA display single scaling. This property has not been investigated before.

To study the self-similarity of the clusters, we used the method based on a moment analysis of the radii of gyration of these clusters [16–18]. In this method the distribution of the cluster radii of gyration is generated for clusters of sizes larger than $s=50$ collected from the 50 simulations at each value of ϕ and x. The moments of the distribution are defined as

$$\sigma_p(R_{g_i}) = \frac{1}{n_i} \sum_{s=1}^{n_i} |R_{g_{i_s}} - \langle R_g \rangle|^p, \tag{1}$$

where n_i is the number of clusters in the ith bin and $\langle R_g \rangle$ is the mean radius of gyration in that bin. Note that $\sigma_p \sim N_i^{p/d_f}$ if $R_{g_{i_s}} \sim N_{i_s}^{1/d_f}$. Therefore, if the system is characterized by one fractal dimension, then the ratio of $\ln(\sigma_p)$ to $\ln(\sigma_q)$ should be equal to p/q for all bins. A deviation from this value indicates multifractality. Our results for BDLCA and IBDLCA are shown in Tables I and II for different mole fractions x. As seen from the tables, the calculated ratios $\ln(\sigma_p)/\ln(\sigma_q)$ are indeed equal to p/q. The uncertainties listed in these tables correspond to twice the standard deviation. From this analysis we conclude that the clusters are self-similar at the three concentrations considered in this work.

Having shown that the clusters are self-similar at all concentrations ϕ and mole fractions x, we present results for the fractal dimension in BDLCA and IBDLCA at different concentrations and mole fractions. There are various methods to determine the fractal dimension d_f [14,18]. In this work we

TABLE I. BDLCA. Slopes of the $\ln \sigma_p$ vs $\ln \sigma_q$ plots for different values of p and q at $\phi=0.01$ and 0.05, and $x=0.2$ and 0.5. Only clusters containing more than 50 monomers were considered.

		$\phi=0.01$		$\phi=0.05$	
p	q	$x=0.2$	$x=0.5$	$x=0.2$	$x=0.5$
3	2	1.50 ± 0.02	1.50 ± 0.01	1.52 ± 0.04	1.48 ± 0.02
4	2	1.99 ± 0.04	1.99 ± 0.02	2.04 ± 0.07	1.95 ± 0.05
5	2	2.49 ± 0.06	2.49 ± 0.04	2.56 ± 0.11	2.42 ± 0.08
4	3	1.33 ± 0.01	1.33 ± 0.02	1.35 ± 0.02	1.32 ± 0.02
5	3	1.67 ± 0.02	1.66 ± 0.01	1.69 ± 0.03	1.64 ± 0.03
5	4	1.25 ± 0.01	1.25 ± 0.00	1.26 ± 0.01	1.24 ± 0.01

TABLE II. IBDLCA. Slopes of the $\ln \sigma_p$ vs $\ln \sigma_q$ plots for different values of p and q at $\phi=0.03$, and $x=0.2$, 0.5, and 0.9. Only clusters containing more than 50 monomers were considered.

p	q	$x=0.2$	$x=0.5$	$x=0.9$
3	2	1.50 ± 0.01	1.51 ± 0.03	1.50 ± 0.02
4	2	2.00 ± 0.03	2.01 ± 0.06	2.00 ± 0.05
5	2	2.50 ± 0.05	2.52 ± 0.11	2.51 ± 0.09
4	3	1.33 ± 0.01	1.34 ± 0.02	1.34 ± 0.02
5	3	1.67 ± 0.02	1.67 ± 0.04	1.67 ± 0.03
5	4	1.25 ± 0.01	1.25 ± 0.01	1.25 ± 0.01

use the mass-size relationship $R_g \sim N^{1/d_f}$, where $1/d_f$ is the slope of the log-log plot of R_g versus N. To avoid large fluctuations due to very small clusters, in the determination of d_f, clusters containing more than 50 monomers were considered.

Illustrated in Fig. 1(a) is the fractal dimension for BDLCA as a function of x for the three concentrations $\phi=0.01$, 0.03, and 0.05. Data points represent averages over 50 simulations and the error bars are twice the standard deviation. As was observed in previous studies of the one-component system [13,14], the fractal dimension increases with concentration ϕ. Additionally, in BDLCA the dependence on molar fraction x is symmetric and the figure illustrates only half of the range of possible molar fractions. In that range the fractal dimension decreases as x increases. In fact, for each ϕ, the fractal dimension approaches a value close to the reaction-limited cluster-cluster aggregation (RLCA) value of the one-component system [13] in the limit of small x, while at $x=0.5$ it becomes close to the diffusion-limited cluster-cluster aggregation (DLCA) value of the one-component system [13]. For example, for the case $\phi=0.01$, we have $d_f=2.07$ at $x=0.2$ and $d_f=1.91$ at $x=0.5$. These values are comparable to the reported values [13] of 2.12 and 1.89 for the RLCA and the DLCA, respectively. The behavior for small x is expected because the small number of A monomers are being consumed rapidly, lying inside the clusters surrounded mostly by B particles, effectively reducing the probability for reaction between colliding clusters, which eventually reaches zero. In fact, an equivalent way to see this phenomenon is to look at the probability of encounters between monomers of different (or alike) species. Figure 1(b) shows the probability of encounters between monomers of the two species as a function of the aggregation time for the four molar fractions x. This probability is a measure of the reactivity in the aggregation bath and is defined as

$$P_R(AB)=\frac{\text{No. of reactive encounters between } A \text{ and } B \text{ monomers}}{\text{total number of encounters}}. \tag{2}$$

The strong decay of the probability for encounters AB as the reaction proceeds in time and the molar fraction x decreases is clearly seen in Fig. 1(b). However, $P_R(AB)$ remains fairly constant in time for $x_A=0.5$ and therefore at this molar fraction the binary mixture behaves much like a one-species system with very small hindrance effects due to the second species. Notice that $P_R(AB)$ is not equivalent to an *effective probability* defined as $2x(1-x)$, which would keep constant during the aggregation process. Instead, even at the onset of the process (initial times), $P_R(AB)$ is smaller than that value because of a kinetic correlation that develops along the aggregation process. The correlation along the reaction time increases, especially for small molar fractions, in such a way that $P_R(AB)$ decreases sharply at the larger times.

The fractal dimension as a function of the mole fraction of the A species for IBDLCA is plotted in Fig. 2(a) for different volume fractions. A behavior similar to that of BDLCA is observed. Overall, the fractal dimension increases with concentration. This model is not symmetric and, for $x>0.5$, the fractal dimension reaches the DLCA value of the one-species case. Otherwise, the fractal dimension becomes close to the RLCA limit of the one-species system as the mole fraction x is decreased. The values of the fractal dimension are somehow larger than those in BDLCA because of a different correlation between reactive particles along the aggregation process. In fact, this difference is apparent even at the beginning of the process because the probability of reacting encounters $P_R(AB)$ is now supplemented by the probability of encounters between A particles:

$$P_R(AA)=\frac{\text{No. of reactive encounters between two } A \text{ monomers}}{\text{total number of encounters}}. \tag{3}$$

The total reaction probability is now $P_R(AA)+P_R(AB)$, which is illustrated in Fig. 2(b) as a function of time.

Summarizing, with respect to structural characteristics, BDLCA and IBDLCA are very similar at $x=0.5$, BDLCA is symmetric, whereas IBDLCA is not. At low x, d_f is higher in IBDLCA indicating the possibility to form slightly more compact clusters.

IV. KINETICS OF THE AGGREGATION PROCESS AND SCALING

The kinetics of aggregating systems is usually studied by monitoring the time evolution of the mean number of clusters $N_c(t)$ or its inverse the number-average cluster size $S_n(t)$, the weight-average cluster size $S_w(t)$, and the cluster-size distribution function $N_s(t)$. The variation with time of $N_c(t)$ and $S_w(t)$ for the BDLCA and the IBDLCA models was investigated at the three concentrations ϕ and different molar fractions x. Figure 3 shows plots of these quantities for BDLCA at $\phi=0.01$ and different molar fractions x. Except for $x=0.2$, these quantities display an exponential behavior at the early times of aggregation, followed apparently by a power-law temporal regime. However, at higher concentrations $\phi=0.03$ and 0.05 the crossover to the power-law regime was not discovered. The IBDLCA model shows a similar behavior for $N_c(t)$ and $S_w(t)$ for $\phi=0.01$ as illustrated in Fig. 4. Our simulations end just before gelation, from where we can infer that the total aggregation time increases as x decreases. Overall, the aggregation time in IBDLCA is a bit larger than in the BDLCA at $x=0.2$ and they become equal at $x=0.5$.

The time dependence of dynamical quantities such as $N_c(t)$ and $S_w(t)$ is characterized by dynamical exponents. The exponents $z'(x)$ and $z(x)$ are obtained as the slopes of the linear regions in the log-log plots of $N_c(t)$ and $S_w(t)$

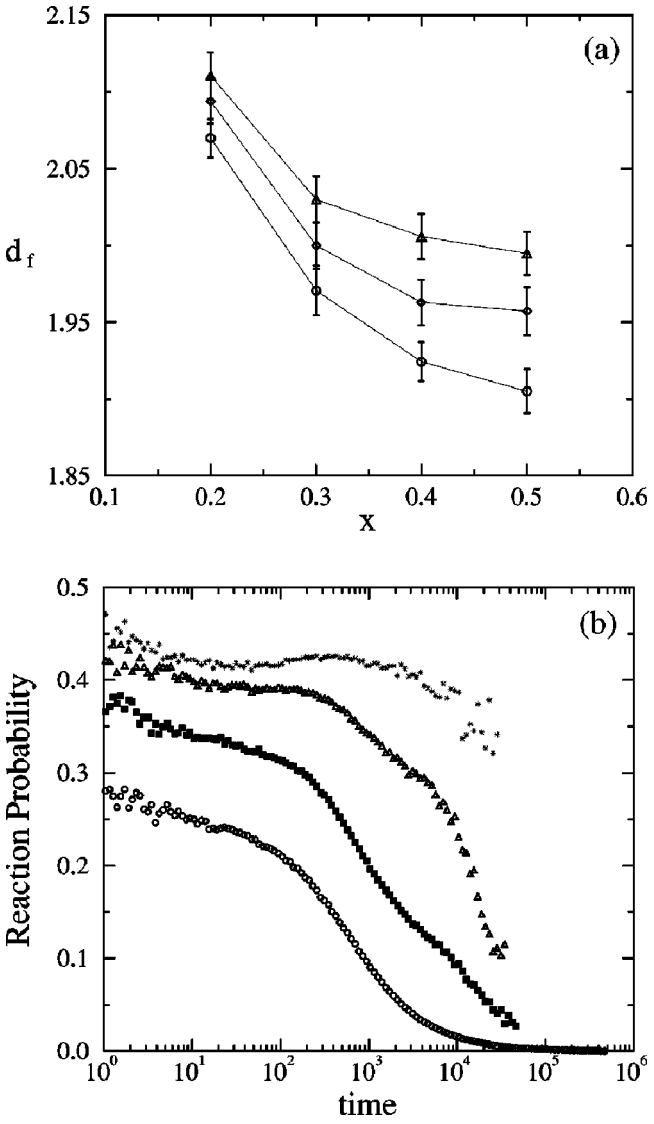

FIG. 1. The BDLCA model. (a) Fractal dimension vs the molar fraction x at $\phi=0.01$ (circles), 0.03 (diamonds), and 0.05 (triangles). (b) Reaction probability P_R as a function of time at $\phi=0.01$ and $x=0.2$ (circles), 0.3 (squares), 0.4 (triangles), and 0.5 (asterisks).

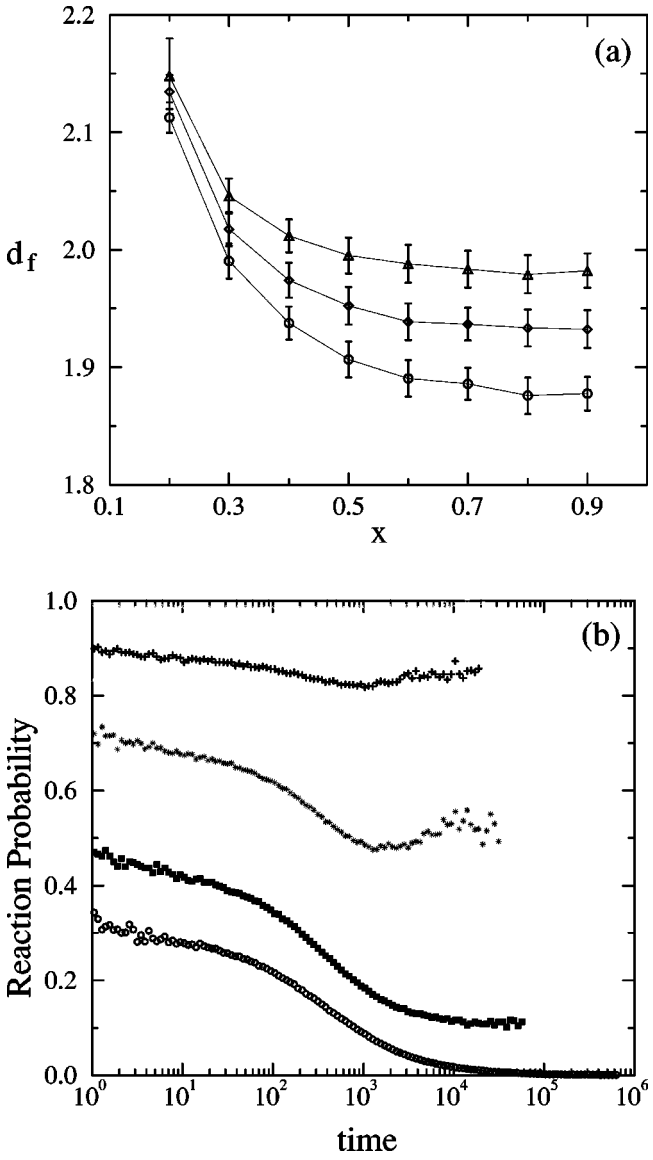

FIG. 2. The IBDLCA model. (a) Fractal dimension vs the molar fraction x at $\phi=0.01$ (circles), 0.03 (diamonds), and 0.05 (triangles). (b) Reaction probability P_R as a function of time at $\phi=0.01$ and $x=0.2$ (circles), 0.3 (squares), 0.5 (asterisks), and 0.7 (crosses).

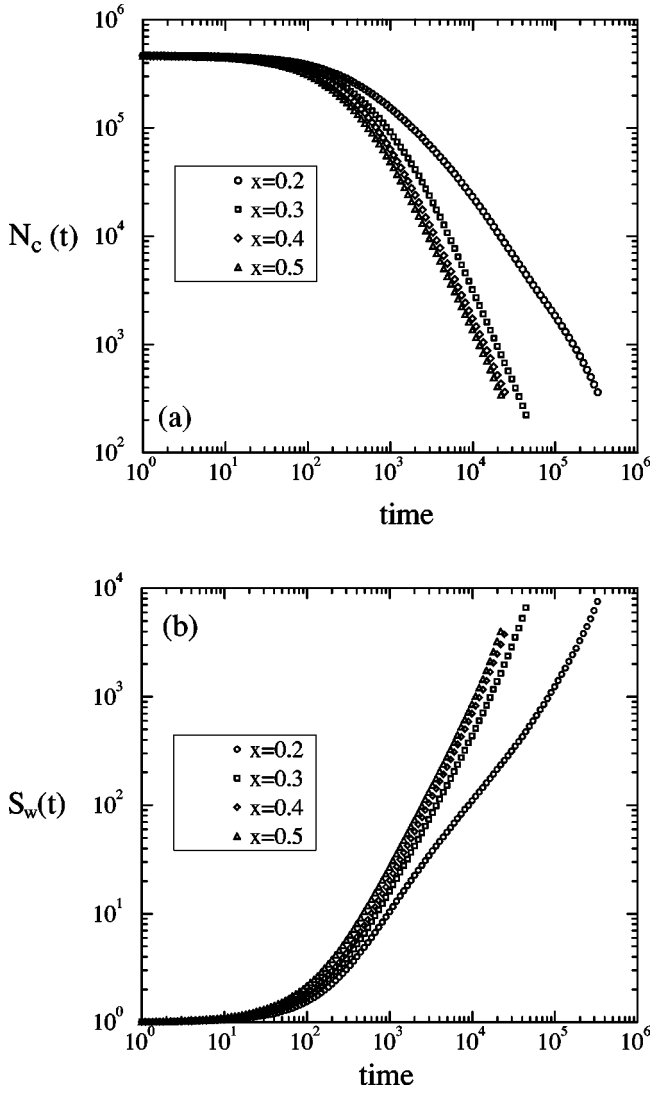

FIG. 3. BDLCA: (a) Mean number of clusters $N_c(t)$ as a function of time. (b) Weight-average cluster size $S_w(t)$ as a function of time. Both plots are for $\phi=0.01$ and various molar fractions x.

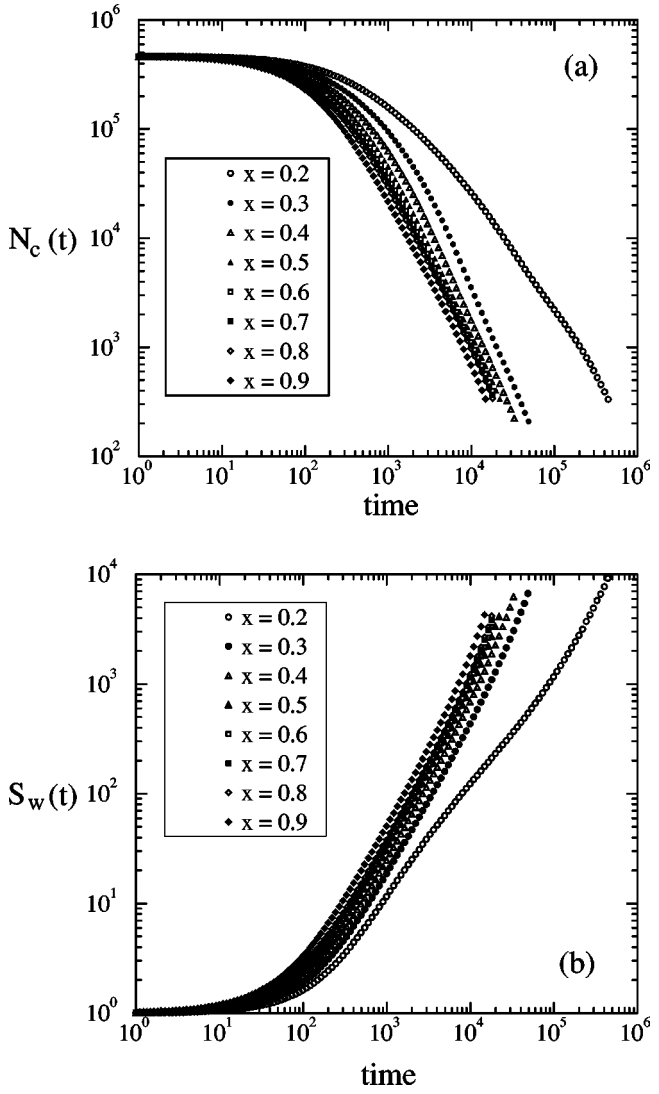

FIG. 4. IBDLCA: (a) Mean number of clusters $N_c(t)$ as a function of time. (b) Weight-average cluster size $S_w(t)$ as a function of time. Both plots are for $\phi=0.01$ and various molar fractions x.

(Figs. 3 and 4), respectively. Values for the exponents are given in Table III for the two models, for $x>0.2$ and $\phi=0.01$. No exponents could be determined at higher concentrations, which is a known problem even for the one-component systems due to finite concentration effects [13]. Notice that while the exponent z does not depend on x, the exponent z' depends slightly on x. The fact that z is constant means that clusters of approximately equal sizes are generated at the same rate irrespective of the value of x, while the change of z' with x means that the rate of decay of clusters is decreasing with increasing x.

Both BDLCA and IBDLCA at about $x=0.2$ display a crossover to a different aggregation regime apparent at the three concentrations under study. Let us emphasize that while the dynamical exponents $z(x)$ and $z'(x)$ were detectable for $x>0.2$, they cannot be obtained for $x\leqslant 0.2$. This abrupt change of behavior can be better explained in terms of the cluster distribution function $N_s(t)$. Figure 5 shows the log-log plots of $N_s(t)$ as a function of time for $x=0.2$ and $x=0.3$. In the case of $x=0.2$, at the early time stages most of the A particles are surrounded by B particles, eventually forming small clusters of different sizes. Among these, there are several fully saturated clusters that do not react during the remaining aggregation time. The lifetime of these nonreactive clusters with sizes of $s=7,12,13,\ldots,$etc. becomes infinite, and for that reason we call them ''metastable clus-

TABLE III. Values of the dynamical exponents z and z' as a function of the molar fraction x for BDLCA and IBDLCA at $\phi=0.01$.

	BDLCA		IBDLCA	
x	z	z'	z	z'
0.3	1.43	1.73	1.34	1.77
0.4	1.49	1.67	1.39	1.69
0.5	1.48	1.62	1.37	1.61
0.6			1.37	1.56
0.7			1.38	1.50
0.8			1.36	1.50
0.9			1.37	1.50

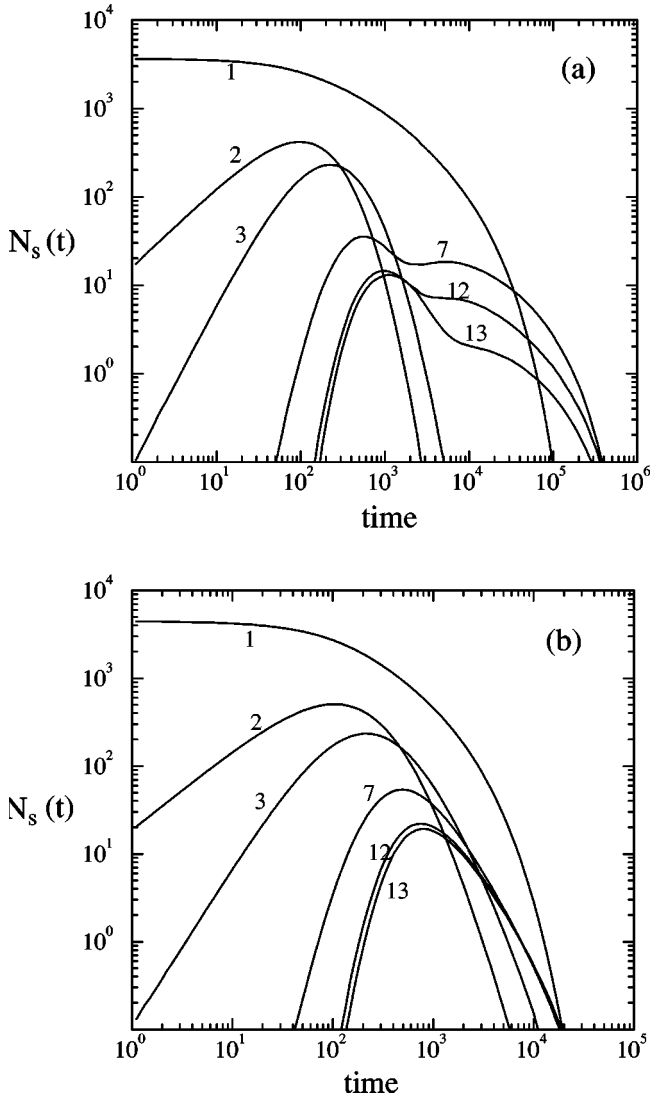

FIG. 5. Time evolution of clusters of size $s=1,2,7,12,$ and 13 for BDLCA at (a) $x=0.2$, (b) $x=0.3$.

ters.'' The specific sizes of the metastable clusters is a characteristic of the simple-cubic lattice model used in this simulation, where each monomer has a functionality of 6 (forming six bonds at most). Systems with different functionalities were not studied here, although lower functionality of 2 and 4 have been studied in the context of polymers [4].

Formation of metastable clusters occurs also for $x>0.2$. However, in these cases they are not abundant enough as to play a significant role in changing the dynamical behavior of the system. When $x\approx 0.2$, we observe a sharp depletion of dimers and trimers which accrue the metastable clusters increasing their number. The rate of formation of these metastable clusters is faster than its rate of annihilation giving rise to a bimodal distribution of metastable clusters of a given size, as seen in Fig. 5(a). At the late aggregation stages the bath is full of metastable clusters, being one of the dominant causes for the aggregation process to slow down and the reaction probability to go to zero [see Figs. 1(b) and 2(b)]. For $x=0.18$, the bimodal distribution flattens to a plateau at long times, indicating the permanent presence in the aggregation time of a third species, namely unreactive metastable clusters. On the other hand, the bimodal behavior is not seen

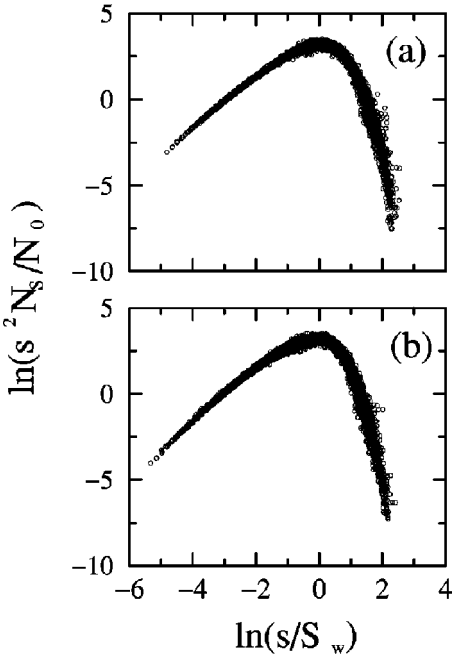

FIG. 6. Scaling at $\phi=0.01$ and $x=0.5$ at 50 different times: (a) BDLCA; (b) IBDLCA.

in Fig. 5(b) for $x=0.3$ and it was not obtained for $x=0.25$ either. This would mean that $x=x_c\approx 0.2$ (between 0.190 and 0.195 for $\phi=0.03$) is a critical point separating two different regimes of aggregation: for $x>x_c$, reactive clusters lead to gelation, and for $x<x_c$, the metastable clusters hinder and inhibit gelation. Meakin and Djordjević [4] predicted this transition, based on observations of a small system (8 000 monomers). According to their interpretation, the system crosses over from a critical to a tricritical behavior [19]. Morover, since our simulations consist of systems of about 470 000 particles, we were able to show that the exponent z is fairly constant in one regime of aggregation, and is not defined in the other regime. This is a sharp transition, whereas in Ref. [4] because of the small system size, a smooth transition was obtained. In light of our results, we can ensure that a phase transition exists in three dimensions similar to a percolation transition [20] where the mole fraction x is related to the occupation probability, the order parameter is the gel fraction (fraction of monomers in the gel), and other relevant quantities are the mean cluster size and the correlation length (spatial extension of the connectivity) [21].

Finally we have checked for scaling of the cluster distribution function $N_s(t)\sim s^{-2}f[s/S_w(t)]$. This is important because it has been detected experimentally for the one-component system [22]. The occurrence of scaling means that when $s^2N_s(t)$ is plotted as a function of $s/S_w(t)$, the distributions collapse onto one master curve for all times in the scaling regime. Figures 6(a) and 6(b) show the collapse of data for BDLCA and IBDLCA at different time windows. The shape of $f(s/S_w)$ is the same for the two models at all values of $x>0.2$ and for the three concentrations ϕ. Early times were not included in the scaling to remove transients of the initial distribution. Similarly, late times were not included because of the statistical fluctuations due to fewer large clusters. The scaling includes cluster sizes $5<s<500$

also for statistical purposes. Worth noticing is that Meakin and Djordjević [4] did not find good collapse for their data because of the apparent curvature in the $S_w(t)$, the small size of the system, and the short time scales that this limitation entails.

V. CONCLUSION

In this paper, we have investigated the influence of the composition x and the volume fraction ϕ on the structural and dynamical properties for aggregation in binary colloidal mixtures. The BDLCA model represents a considerable improvement on the simulation approach of previous studies [4,6] (two orders of magnitude more monomers, longer aggregation times, better statistics). Additionally, the kinetic behavior is better suited for comparison to experiments because clusters exhibit size-dependent mobilities. The invasion binary diffusion-limited aggregation, IBDLCA, is a newly introduced model that presents several differences with BDLCA and is prone to represent alternative experimental situations that allow for bonding between one of the species.

In both models, increasing the molar fraction x decreases the fractal dimension and increases the reaction probability, which drives the d_f from the RLCA to the DLCA limits of the one-monomer system. With respect to x, BDLCA is regarded as symmetric whereas IBDLCA is asymmetric. In both models, the fractal dimension increases with increasing concentration ϕ. At the lowest concentration considered here ($\phi=0.01$) and for $x>0.2$, the exponent z associated with the weight-average cluster size $S_w(t)$ and the exponent z' associated with the number-average cluster size $S_n(t)$ are defined. The first exponent remains fairly constant while z' presents a slight decrease with increasing x. No power-law behavior was obtained for higher values of ϕ, notwithstanding that scaling in the form $N_s(t)\sim s^{-2}f[s/S_w(t)]$ was found. In IBDLCA saturation is reached whenever the invading monomers are a minority ($x>0.5$), i.e., the fractal dimension and the dynamical exponents z and z' tend to some constants, close to the characteristic values of the one-component systems [13]. In both models the point $x\approx 0.2$ is found to be a critical point separating the gelling from the nongelling regimes.

ACKNOWLEDGMENTS

E.B.B. acknowledges partial support for this work from Grant No. CTS-9806321 of the National Science Foundation. A.S. is supported by the Saudi Arabia government. A.E.G. acknowledges partial support from CONACYT (Mexico) Grants No. 3165-PE and No. E120.1381.

[1] *Kinetics of Aggregation and Gelation*, edited by F. Family and D. P. Landau (Elsevier, Amsterdam, 1984).
[2] R. Jullien and R. Botet, *Aggregation and Fractal Aggregates* (World Scientific, Singapore, 1987).
[3] T. Vicsek, *Fractal Growth Phenomena* (World Scientific, Singapore, 1989).
[4] P. Meakin and Z. B. Djordjević, J. Phys. A **19**, 2137 (1986).
[5] P. Meakin and S. Miyazima, J. Phys. Soc. Jpn. **57**, 4439 (1988).
[6] S. Stoll and E. Pefferkorn, J. Colloid Interface Sci. **160**, 149 (1993).
[7] S. Stoll and E. Pefferkorn, J. Colloid Interface Sci. **177**, 192 (1996).
[8] G. K. von Schulthess, G. B. Benedek, and R. W. de Blois, Macromolecules **13**, 939 (1980).
[9] S. K. Friedlander, *Smoke, Dust and Haze: Fundamentals of Aerosol Behavior* (Wiley, New York, 1977).
[10] C. A. Morris, M. L. Anderson, R. M. Stroud, C. I. Merzbacher, and D. R. Rolison, Science **284**, 622 (1999).
[11] M. Yasrebi, W. Y. Shih, and I. A. Aksay, J. Colloid Interface Sci. **142**, 357 (1991).
[12] P. Meakin, T. Vicsek, and F. Family, Phys. Rev. B **31**, 564 (1985).
[13] M. Lach-hab, A. E. González, and E. Blaisten-Barojas, Phys. Rev. E **54**, 5456 (1996).
[14] A. E. González, M. Lach-hab, and E. Blaisten-Barojas, J. Sol-Gel Sci. Technol. **15**, 119 (1999).
[15] C. Amitrano, A. Coniglio, P. Meakin, and M. Zannetti, Phys. Rev. B **44**, 4974 (1991).
[16] B. B. Mandelbrot, H. Kaufman, A. Vespignani, I. Yekutieli, and C. H. Lam, Europhys. Lett. **29**, 599 (1995).
[17] D. Queiros-Conde, Phys. Rev. Lett. **78**, 4426 (1997).
[18] M. Lach-hab, A. E. González, and E. Blaisten-Barojas, Phys. Rev. E **57**, 4520 (1998).
[19] E. K. Riedel and F. J. Wegner, Phys. Rev. Lett. **29**, 349 (1972).
[20] D. Stauffer and A. Aharony, *Percolation Theory* (Taylor and Francis, London, 1992), p. 57.
[21] A. AlSunaidi, E. Blaisten-Barojas, and A. E. González (unpublished).
[22] M. Broide and R. J. Cohen, Phys. Rev. Lett. **64**, 2026 (1990).